Density Functional Theory Study of Aqueous-Phase Rate Acceleration and *Endo/Exo* Selectivity of the Butadiene and Acrolein Diels−Alder Reaction

Sue Kong and Jeffrey D. Evanseck*,†

Contribution from the Department of Chemistry, University of Miami, 1301 Memorial Drive, Coral Gables, Florida 33146-0431, and Department of Chemistry and Biochemistry, Duquesne University, 600 Forbes Avenue, Pittsburgh, Pennsylvania 15282-1530

Received March 22, 2000

Abstract: The four stereospecific transition structures of the butadiene and acrolein Diels−Alder reaction have been studied using the Becke three-parameter density functional theory with the 6-31G(d) basis set. The effect of solvent on the activation energies and *endo/exo* selectivity has been approximated by the polarizable continuum model (PCM); explicit definition of one, two, and three waters; and the combined strategy of the discrete-continuum model. The full aqueous acceleration and enhanced *endo/exo* selectivity observed by experiment is computed only when solvation forces are approximated by the discrete-continuum model. Consistent with previous ideas, two explicit waters are used to satisfy localized hydrogen bonding of acrolein and induce a charge polarization of the *endo s-cis* transition structure. Smaller enforced hydrophobic interactions result. Significant bulk-phase effects beyond hydrogen bonding and enforced hydrophobic interactions are computed for the first time. The gas-phase activation energy is lowered to 11.5 kcal/mol, in excellent agreement with known experimental activation energies of similar Diels−Alder reactions in mixed methanol and water solutions. The computed *endo* preference is enhanced to 2.4 kcal/mol in aqueous solution, in agreement with experiment. Approximately 50% of the rate acceleration and *endo/exo* selectivity is attributed to hydrogen bonding, and the remainder to bulk-phase effects, which includes enforced hydrophobic interactions and antihydrophobic cosolvent effects. The local and bulk influence of solvent on the energetics, *endo/exo* selectivity, and transition structure asynchronicity is discussed and analyzed for this particular pericyclic reaction that has a well-known and strong solvent dependency. The catalytic and *endo/exo* selectivity results are consistent with the hypothesis of maximum accumulation of unsaturation and support the importance of antihydrophobic cosolvents in stabilizing hydrophobic regions of transition structures.

Introduction

The Diels−Alder reaction is one of the most important and widely used carbon−carbon bond-forming processes in organic chemistry.[1−7] Due to the broad scope and proven usefulness of the Diels−Alder reaction, there have been extensive efforts to control the rate and regio, *endo/exo*, and diastereofacial selectivities by using the aqueous phase.[8−12] Generally, pericyclic reactions are regarded as concerted and nearly synchronous reactions[13,14] that have insignificant charge build-up in their corresponding transition structures.[15] As a result, it is commonly thought that many pericyclic reaction rates and stereoselectivities remain unaffected by solvent.[16−19] Despite the assumption of a relatively static charge distribution, it is now well-established that several reactions from different pericyclic classifications, such as the Diels−Alder reaction,[20−29] hetero-Diels−Alder reaction,[30−33] 1,3-dipolar cycloaddition,[34−39] Claisen rearrange-

* To whom correspondence should be addressed.
† Duquesne University.

(1) Oppolzer, W. In *Intermolecular Diels−Alder Reactions*; Trost, B. M., Ed.; Pergamon Press: Oxford, 1991; Vol. 5, p 315.
(2) Weinreb, S. M. In *Heterodienophile Additions to Dienes*; Trost, B. M., Ed.; Pergamon Press: Oxford, 1991; Vol. 5, p 401.
(3) Boger, D. L. In *Heterodiene Additions*; Trost, B. M., Ed.; Pergamon Press: Oxford, 1991; Vol. 5, p 451.
(4) Roush, W. R. In *Intramolecular Diels−Alder Reactions*; Trost, B. M., Ed.; Pergamon Press: Oxford, 1991; Vol. 5, p 513.
(5) Sweger, R. W.; Czarnik, A. W. In *Retrograde Diels−Alder Reactions*; Trost, B. M., Ed.; Pergamon Press: Oxford, 1991; Vol. 5, p 551.
(6) Carruthers, W. *Cycloaddition Reactions in Organic Synthesis*; Pergamon Press: New York, 1990.
(7) Fringuelli, F.; Tatichi, A. *Dienes in the Diels−Alder Reaction*; Wiley: New York, 1990.
(8) Lubineau, A.; Auge, J. *Top. Curr. Chem.* **1999**, *206*, 1.
(9) Lubineau, A.; Auge, J.; Queneau, Y. *Synthesis* **1994**, 741.
(10) Pindur, U.; Lutz, G.; Otto, C. *Chem. Rev.* **1993**, *93*, 741.
(11) Li, C.-J. *Chem. Rev.* **1993**, *93*, 2023, and references therein.
(12) Grieco, P. A. *Organic Synthesis in Water*; Blackie Academic and Professional: London, 1998.
(13) Houk, K. N.; González, J.; Li, Y. *Acc. Chem. Res.* **1995**, *28*, 81.
(14) Houk, K. N.; Li, Y.; Evanseck, J. D. *Angew. Chem., Int. Ed. Engl.* **1992**, *31*, 682.
(15) Sauer, J.; Sustmann, R. *Angew. Chem., Int. Ed. Engl.* **1980**, *19*, 779.
(16) Reichardt, C. *Solvents and Solvent Effects in Organic Chemistry*, 2nd ed.; VCH: Weinheim, 1988.
(17) Gajewski, J. J. *J. Org. Chem.* **1992**, *57*, 5500.
(18) Desimoni, G.; Faita, G.; Pasini, D.; Righetti, P. P. *Tetrahedron* **1992**, *48*, 1667.
(19) Huisgen, R. *Pure Appl. Chem.* **1980**, *52*, 2283.
(20) Garner, P. P. In *Diels−Alder Reactions in Aqueous Media*; Grieco, P. A., Ed.; Blackie Academic and Professional: London, 1998.
(21) Meijer, A.; Otto, S.; Engberts, J. B. F. N. *J. Org. Chem.* **1998**, *63*, 8989.
(22) Wijnen, J. W.; Engberts, J. B. F. N. *J. Org. Chem.* **1997**, *62*, 2039.
(23) van der Wel, G. K.; Wijnen, J. W.; Engberts, J. B. F. N. *J. Org. Chem.* **1996**, *61*, 9001.
(24) Engberts, J. B. F. N. *Pure Appl. Chem.* **1995**, *67*, 823.
(25) Otto, S.; Blokzijl, W.; Engberts, J. B. F. N. *J. Org. Chem.* **1994**, *59*, 5372.

10.1021/ja0010249 CCC: $19.00
Published on Web 10/07/2000

ment,[40−43] and aldol[44] and benzoin condensations,[45−47] are strongly accelerated in aqueous medium. In particular, the rates of Diels−Alder reactions have been accelerated by factors up to 1.3×10^4 in aqueous solution as compared to organic solvents.[24,25]

A review of theoretical studies to understand the role of solvent on the rate acceleration and stereoselectivity of the Diels−Alder reaction has been recently reported.[48] The self-consistent reaction-field (SCRF) continuum approach, coupled with semiempirical molecular orbital theories such as MINDO/3, PM3, and AM1, has been applied to different Diels−Alder reactions with various degrees of success.[49−52] The interpretations are complicated by the preference of MINDO/3 for the biradical stepwise mechanism and the lack of transition structure charge separation by AM1.[42,49] In addition, Hartree−Fock theory has been combined with SCRF models to study solvation effects on different Diels−Alder reactions.[32,33,53] Despite the success of Hartree−Fock in modeling Diels−Alder reactions in a vacuum,[13,14,54,55] the importance of including electron correlation in activated systems has been demonstrated.[56−59] Specifically, the *endo s-cis* Lewis acid-catalyzed butadiene and acrolein transition structure, computed using Hartree−Fock and a spliced 6-31G(d) and 3-21G basis set, corresponds to a [2 + 4] hetero Diels−Alder reaction, instead of the expected [4 + 2] cycloaddition.[60] Inclusion of electron correlation in the geometry optimization process using Møller−Plesset or density functional theories provides a correct [4 + 2] description of transition structure geometries and energies for this particular cycloaddition.[56,59] Because polar solvent is thought to activate the dienophile in a manner similar to that of a Lewis acid, the inclusion of electron correlation is necessary in this study. Furthermore, an SCRF solvation model using an ellipsoidal cavity shape and a hexapole reaction field, combined with MP2/6-31G(p,d) energy evaluations on RHF/3-21G-optimized structures, was used to describe the solvation effects on the cyclopentadiene and methyl acrylate Diels−Alder reaction.[53] Instead of the expected catalytic effect, the computed electrostatic effects in water were found to raise slightly the Gibbs energy of activation, which was rationalized by underestimated hydrophobic effects and the inability of the model to accommodate explicit hydrogen bonding.[53] Therefore, intrinsic difficulties with previously applied SCRF approximations, in either the Hamiltonian or continuum implementation, have averted meaningful interpretations of activation-barrier decreases and greater *endo/exo* selectivities with increasing solvent polarity.[48]

An extensive body of recent experimental[20−29] and computational[54,55,61−63] data yields insight into the factors responsible for the aqueous acceleration and increased *endo/exo* selectivities of Diels−Alder reactions. Two primary effects involve "enhanced hydrogen bonding" between the solvent and the transition structure relative to the initial state,[22−26,28] and "enforced hydrophobic interactions" as the reactant hydrophobic surface area decreases during the activation process.[21,27,29] Recent research has been aimed at separating and quantifying the relative contribution of each interaction type to aqueous acceleration.[20−29,61−63] Jorgensen and co-workers have set the stage to better understand enhanced hydrogen bonding effects by employing an explicit treatment of solvent using the OPLS force-field and Monte Carlo simulations.[63] Jorgensen computed the Gibbs energy of solvation (ΔG_{sol}) for the cyclopentadiene and methyl vinyl ketone Diels−Alder reaction.[54,63] Analysis of the simulations revealed ca. 2−2.5 hydrogen bonds with the dienophile along the reaction coordinate. The polarized carbonyl group produced stronger hydrogen bonds (1−2 kcal/mol per hydrogen bond) at the transition structure. Thus, the aqueous acceleration was found to contain a significant nonhydrophobic component stemming from the enhanced polarization of the transition structure. Ab initio calculations with a single water molecule support the idea that the observed rate accelerations for Diels−Alder reactions arise from the hydrogen bonding effect, in addition to a relatively constant hydrophobic contribution (factor of ca. 10 on the rate).[54,63] However, the special effect of water on Diels−Alder reactions, beyond hydrogen bonding, has been shown by the reduced rate constants in fluorinated

(26) Blokzijl, W.; Engberts, J. B. F. N. In *Enforced Hydrophobic Interactions and Hydrogen Bonding in the Acceleration of Diels−Alder Reactions in Water*; Cramer, C. J., Truhlar, D. G., Eds.; American Chemical Society: Washington, DC, 1994; Vol. 568, p 303.
(27) Blokzijl, W.; Engberts, J. B. F. N. *Angew. Chem., Int. Ed. Engl.* **1993**, *32*, 1545.
(28) Blokzijl, W.; Engberts, J. B. F. N. *J. Am. Chem. Soc.* **1992**, *114*, 5440.
(29) Blokzijl, W.; Blandamer, M. J.; Engberts, J. B. F. N. *J. Am. Chem. Soc.* **1991**, *113*, 4241.
(30) Parker, D. T. In *Hetero Diels−Alder Reaction*; Grieco, P. A., Ed.; Blackie Academic and Professional: London, 1998, and references therein.
(31) Wijnen, J. W.; Zavarise, S.; Engberts, J. B. F. N. *J. Org. Chem.* **1996**, *61*, 2001.
(32) Suárez, D.; Assfeld, X.; González, J.; Ruiz-López, M. F.; Sordo, T. L.; Sordo, J. A. *J. Chem. Soc., Chem. Commun.* **1994**, 1683.
(33) McCarrick, M. A.; Wu, Y.; Houk, K. N. *J. Org. Chem.* **1993**, *58*, 3330.
(34) Gholami, M. R.; Yangjeh, A. H. *J. Chem. Res., Synop.* **1999**, *3*, 226.
(35) van Mersbergen, D.; Wijnen, J. W.; Engberts, J. B. F. N. *J. Org. Chem.* **1998**, *63*, 8801.
(36) Wijnen, J. W.; Steiner, R. A.; Engberts, J. B. F. N. *Tetrahedron Lett.* **1995**, *36*, 5389.
(37) Rohloff, J. C.; Robinson, J.; Gardner, J. O. *Tetrahedron Lett.* **1992**, *33*, 3113.
(38) Inoue, Y.; Araki, K.; Shiraishi, S. *Bull. Chem. Soc. Jpn.* **1991**, *64*, 3079.
(39) Dignam, K. J.; Hegarty, A. F.; Quain, P. L. *J. Org. Chem.* **1978**, *43*, 388.
(40) Gajewski, J. J. In *Claisen Rearrangements in Aqueous Solution*; Grieco, P. A., Ed.; Blackie Academic and Professional: London, 1998, and references therein.
(41) Gao, J. *J. Am. Chem. Soc.* **1994**, *116*, 1563.
(42) Cramer, C. J.; Truhlar, D. G. *J. Am. Chem. Soc.* **1992**, *114*, 8794.
(43) Severance, D. L.; Jorgensen, W. L. *J. Am. Chem. Soc.* **1992**, *114*, 10966.
(44) Kobayashi, S. In *Water-Stable Rare-Earth Lewis-Acid Catalysis in Aqueous and Organic Solutions*; Grieco, P. A., Ed.; Blackie Academic and Professional: London, 1998, and references therein.
(45) Breslow, R.; Connors, R. V. *J. Am. Chem. Soc.* **1995**, *117*, 6601.
(46) Breslow, R. *Acc. Chem. Res.* **1991**, *24*, 159.
(47) Kool, E. T.; Breslow, R. *J. Am. Chem. Soc.* **1988**, *110*, 1596.
(48) Cativiela, C.; García, J. I.; Mayoral, J. A.; Salvatella, L. *Chem. Soc. Rev.* **1996**, 209.
(49) Cativiela, C.; Dillet, V.; García, J. I.; Mayoral, J. A.; Ruiz-López, M. F.; Salvatella, L. *J. Mol. Struct. (THEOCHEM)* **1995**, *331*, 37.
(50) Karcher, T.; Sicking, W.; Sauer, J.; Sustmann, R. *Tetrahedron Lett.* **1992**, *33*, 8027.
(51) Sustmann, R.; Sicking, W. *Tetrahedron* **1992**, *48*, 10293.
(52) Pardo, L.; Branchadell, V.; Oliva, A.; Bertrán, J. *J. Mol. Struct. (THEOCHEM)* **1983**, *93*, 255.
(53) Ruiz-López, M. F.; Assfeld, X.; García, J. I.; Mayoral, J. A.; Salvatella, L. *J. Am. Chem. Soc.* **1993**, *115*, 8780.
(54) Blake, J. F.; Lim, D.; Jorgensen, W. L. *J. Org. Chem.* **1994**, *59*, 803.
(55) Jorgensen, W. L.; Lim, D.; Blake, J. F. *J. Am. Chem. Soc.* **1993**, *115*, 2936.
(56) García, J. I.; Martinez-Merino, V.; Mayoral, J. A.; Salvatella, L. *J. Am. Chem. Soc.* **1998**, *120*, 2415.
(57) Wiest, O.; Montiel, D. C.; Houk, K. N. *J. Phys. Chem. A* **1997**, *101*, 8378.
(58) Goldstein, E.; Beno, B.; Houk, K. N. *J. Am. Chem. Soc.* **1996**, *118*, 6036.
(59) Garcia, J. I.; Mayoral, J. A.; Salvatella, L. *J. Am. Chem. Soc.* **1996**, *118*, 11680.
(60) Yamabe, S.; Dai, T.; Minato, T. *J. Am. Chem. Soc.* **1995**, *117*, 10994.
(61) Furlani, T. R.; Gao, J. *J. Org. Chem.* **1996**, *61*, 5492.
(62) Jorgensen, W. L.; Blake, J. F.; Lim, D.; Severance, D. L. *J. Chem. Soc., Farady Trans.* **1994**, *90*, 1727.
(63) Blake, J. F.; Jorgensen, W. L. *J. Am. Chem. Soc.* **1991**, *113*, 7430.

alcohol solvents, which have a stronger hydrogen bond donor capacity than water.[21,22] Clearly, factors other than hydrogen bonding are in operation.

Breslow first suggested that hydrophobic packing of the diene and dienophile is responsible for observed rate accelerations.[27,46,64−69] Subsequently, Engberts made a distinction between hydrophobic packing and enforced hydrophobic interactions. The term "enforced" is used to stress that hydrophobic interactions are an integral part of the activation process.[21,27,29] As with enhanced hydrogen bonding, the focus is on the relative stabilization between the initial state and the transition structure, which manifests in the available hydrophobic surface area along the reaction coordinate. Concerning mixed solvent systems, Breslow recently reported antihydrophobic cosolvent effects, which is a relationship between reaction rate and inaccessible hydrophobic surface area of the transition structure.[70−73] In brief, an alcohol cosolvent does not interfere with water's ability to stabilize polarizable transition structures; rather, it enhances transition structure solvation by stabilizing hydrophobic regions.[70−72] Since the inception of aqueous rate accelerations and enhanced stereoselectivities of organic reactions,[66] many interpretations beyond enhanced hydrogen bonding and enforced hydrophobic effects have been advanced and recently discussed.[21,74] Most notably are internal pressure,[74−79] cohesive energy density of water,[17,80] micellar,[81−84] and medium polarity and solvophobic effects.[29,85−90] Even though electrostatic effects through enhanced hydrogen bonding between water and the transition structure account for an important part of the Diels−Alder rate acceleration, the remainder of enhanced acceleration by hydrophobic and other effects continue to be controversial and an active area of research.

Given the synthetic importance and current understanding of external effects on the Diels−Alder reaction, it is important to further investigate the dramatic rate acceleration and *endo/exo* selectivity caused by the aqueous phase. To date, a density functional study employing a continuum strategy to describe accurately the effect of the aqueous phase on the Diels−Alder reaction has not been reported. Density functional theory is used to include the effects of electron correlation in determining the transition structures, while the influence of solvent is simultaneously included by continuum, discrete, and combined discrete-continuum models. As a result, a more complete understanding of the aqueous-phase influence through local hydrogen bonding, enforced hydrophobic interactions, and antihydrophobic cosolvent effects on the Diels−Alder reaction is directly computed by a combined density functional theory and the polarizable continuum model (PCM) discrete-continuum method.

Computational Methods

All ab initio and solvation model calculations were carried out with the Gaussian 98 program[91] and by using a 16-node SP IBM RS/6000 super computer.[92] The discrete, continuum, and discrete-continuum solvation models are used to approximate the effect of solvent on the butadiene and acrolein Diels−Alder reaction. The discrete model included explicit water molecules in the quantum mechanical calculations in order to satisfy local hydrogen bonding. One, two, and three waters have been considered separately, because Monte Carlo simulations indicate that ca. 2−2.5 waters hydrogen bond with acrolein along the reaction coordinate.[54]

The Becke three-parameter exchange functional[93] and the nonlocal correlation functional of Lee, Yang, and Parr[94] with the 6-31G(d) basis set[95] has been employed. All energy optimizations, frequency analyses and solvation computations were carried out using the B3LYP/6-31G(d) level of theory, which has been shown to produce realistic structures and energies for pericyclic reactions[57,58] and to treat properly the butadiene and acrolein Diels−Alder gas-phase reaction.[56,59] Vibrational-frequency calculations at the same level of theory were used to confirm all stationary points as either minima or transition structures and to provide thermodynamic and zero-point energy corrections (Supporting Information).

The implicit model involves effective Hamiltonian methods that use continuum distributions to describe the solvent.[96] The advantage of such a scheme is that bulk solvent effects that are calibrated against macroscopic properties can be efficiently included within the quantum mechanical framework.[97] The polarizable continuum model (PCM) by Tomasi and co-workers has been selected,[98−100] because it has been used to investigate successfully the effect of solvent upon the energetics and equilibria of other small molecular systems. The PCM method has been described in detail.[96] Briefly, the solute is represented by a charge

(64) Breslow, R.; Rizzo, C. J. *J. Am. Chem. Soc.* **1991**, *113*, 4340.
(65) Breslow, R.; Guo, T. *J. Am. Chem. Soc.* **1988**, *110*, 5613.
(66) Rideout, D. C.; Breslow, R. *J. Am. Chem. Soc.* **1980**, *102*, 7816.
(67) Breslow, R.; Maitra, U. *Tetrahedron Lett.* **1984**, *25*, 1239.
(68) Breslow, R.; Maitra, U.; Rideout, D. *Tetrahedron Lett.* **1983**, *24*, 1901.
(69) Hunt, I.; Johnson, C. D. *J. Chem. Soc., Perkin Trans. 2* **1991**, 1051.
(70) Breslow, R.; Groves, K.; Mayer, M. U. *Org. Lett.* **1999**, *1*, 117.
(71) Breslow, R.; Connors, R.; Zhu, Z. *Pure Appl. Chem.* **1996**, *68*, 1527.
(72) Breslow, R.; Zhu, Z. *J. Am. Chem. Soc.* **1995**, *117*, 9923.
(73) Breslow, R. *Struct. React. Aqueous Solution* **1994**, *568*, 291.
(74) Pawar, S. S.; Phalgune, U.; Kumar, A. *J. Org. Chem.* **1999**, *64*, 7055.
(75) Grieco, P. A.; Nunes, J. J.; Gaul, M. D. *J. Am. Chem. Soc.* **1990**, *112*, 4595.
(76) Lubineau, A. *J. Org. Chem.* **1986**, *51*, 2142.
(77) Lubineau, A.; Quenau, Y. *J. Org. Chem.* **1987**, *52*, 1001.
(78) Grieco, P. A.; Brandes, E. B.; McCann, S.; Clark, J. D. *J. Org. Chem.* **1989**, *54*, 5849.
(79) Dack, M. R. J. *Chem. Soc. Rev.* **1975**, *4*, 211.
(80) Grieco, P. A. *Tetrahedron Lett.* **1986**, *27*, 1975.
(81) Otto, S.; Engberts, J. B. F. N.; Kwak, J. C. T. *J. Am. Chem. Soc.* **1998**, *120*, 9517.
(82) Yoshida, K.; Grieco, P. A. *J. Org. Chem.* **1984**, *49*, 5257.
(83) Grieco, P. A.; Garner, P.; Zhen-Min, H. *Tetrahedron Lett.* **1983**, *24*, 1897.
(84) Grieco, P. A.; Yoshida, K.; Garner, P. *J. Org. Chem.* **1983**, *48*, 3137.
(85) Cativiela, C.; García, J. I.; Gil, J.; Martínez, R. M.; Mayoral, J. A.; Salvatella, L.; Urieta, J. S.; Mainar, A. M.; Abraham, M. H. *J. Chem. Soc., Perkin Trans. 2* **1997**, 653.
(86) Cativiela, C.; García, J. I.; Mayoral, J. A.; Royo, A. J.; Salvatella, L.; Assfeld, X.; Ruiz-Lopez, M. F. *J. Phys. Org. Chem.* **1992**, *5*, 230.
(87) Cativiela, C.; García, J. I.; Mayoral, J. A.; Avenoza, A.; Peregrina, J. M.; Roy, M. A. *J. Phys. Org. Chem.* **1991**, *4*, 48.
(88) Sangwan, N. K.; Schneider, H.-J. *J. Chem. Soc., Perkin Trans. 2* **1989**, 1223.
(89) Schneider, H.-J.; Sangwan, N. K. *J. Chem. Soc., Chem. Commun.* **1986**, 1787.
(90) Schneider, H.-J.; Sangwan, N. K. *Angew. Chem., Int. Ed. Engl.* **1987**, *26*, 896.
(91) Frisch, M. J.; Trucks, G. W.; Schlegel, H. B.; Scuseria, G. E.; Robb, M. A.; Cheeseman, J. R.; Zakrzewski, V. G.; Montgomery Jr., J. A.; Stratmann, R. E.; Burant, J. C.; Dapprich, S.; Millam, J. M.; Daniels, A. D.; Kudin, K. N.; Strain, M. C.; Farkas, O.; Tomasi, J.; Barone, V.; Cossi, M.; Cammi, R.; Mennucci, B.; Pomelli, C.; Adamo, C.; Clifford, S.; Ochterski, J.; Petersson, G. A.; Ayala, P. Y.; Cui, Q.; Morokuma, K.; Malick, D. K.; Rabuck, A. D.; Raghavachari, K.; Foresman, J. B.; Cioslowski, J.; Ortiz, J. V.; Stefanov, B. B.; Liu, G.; Liashenko, A.; Piskorz, P.; Komaromi, I.; Gomperts, R.; Martin, R. L.; Fox, D. J.; Keith, T.; Al-Laham, M. A.; Peng, C. Y.; Nanayakkara, A.; Gonzalez, C.; Challacombe, M.; Gill, P. M. W.; Johnson, B.; Chen, W.; Wong, M. W.; Andres, J. L.; Gonzalez, C.; Head-Gordon, M.; Replogle, E. S.; Pople, J. A. *Gaussian 98*, Revision A., 3rd ed.; Gaussian, Inc.: Pittsburgh, PA, 1998.
(92) The I.B.M. Corporation is thanked for their commitment to supporting university research and educational activities.
(93) Becke, A. D. *J. Chem. Phys.* **1993**, *98*, 5648.
(94) Lee, C.; Yang, W.; Parr, R. G. *Phys. Rev.* **1988**, *37*, 785.
(95) Petersson, G. A.; Al-Laham, M. A. *J. Chem. Phys.* **1991**, *94*, 6081.
(96) Tomasi, J.; Persico, M. *Chem. Rev.* **1994**, *94*, 2027.
(97) Klamt, A.; Jonas, V. *J. Chem. Phys.* **1996**, *105*, 9972.
(98) Miertus, S.; Scrocco, E.; Tomasi, J. *Chem. Phys.* **1981**, *55*, 117.
(99) Aguilar, M. A.; Olivares del Valle, F. J.; Tomasi, J. *Chem. Phys.* **1993**, *98*, 7375.
(100) Cossi, M.; Barone, V.; Cammi, R.; Tomasi, J. *Chem. Phys. Lett.* **1996**, *255*, 327.

distribution in a cavity embedded in an infinite polarizable dielectric medium. The cavity shape is obtained from the van der Waals radii of the atoms of the solute. The solvents and dielectric constants used in this study are benzene ($\epsilon = 2.25$), methylene chloride ($\epsilon = 8.93$), methanol ($\epsilon = 32.0$), and water ($\epsilon = 78.4$). Full geometry optimizations were carried out for the discrete and PCM models. To account simultaneously for localized hydrogen bonding and bulk solvation effects, single point energy calculations using the discrete-continuum procedure have been employed using PCM on the geometry-optimized two-discrete-water structures. It is known that continuum methods, such as PCM, neglect the effect of entropy.[100] Contributions due to thermal, vibrational, rotational, and translational motions, including zero-point energies, are included separately by standard statistical mechanical procedures available in Gaussian 98. Consequently, this study targets the direct comparison between computed and experimental activation energies[101] and activation enthalpies.[102]

The Mulliken overlap population has been used to gauge the strength of noncovalent bonding.[103,104] This indicator is known to be basis-set-dependent and is subject to many criticisms. Nevertheless, the Mulliken population overlap has been previously used to understand important secondary orbital interactions that occur at transition structures.[105−108] To determine the atomic charges, the CHELPG algorithm, developed by Breneman and Wiberg, has been used.[109] It combines the regular grid of points of Cox and Williams[110] with the Lagrange multiplier method of Chirlian and Francl that was employed in CHELPG.[111] In CHELPG, a cubic grid of points (spaced 0.3−0.8 Å apart) is used, and all grid points that lie within the van der Waals radius of any atom are discarded, together with all points that lie more than 2.8 Å away from any atom. CHELPG charges with 6-31G(d) basis set in all-atom format have been previously shown to be more reliable than the Mulliken charges in solvent simulations.[112]

Results and Discussion

Four possible reaction pathways are possible for the Diels−Alder reaction between acrolein and *s-cis* butadiene. Consistent with previous conventions,[56,106] the transition structures are denoted as NC (*endo*, *s-cis* acrolein), XC (*exo*, *s-cis* acrolein), NT (*endo*, *s-trans* acrolein) and XT (*exo*, *s-trans* acrolein), as shown in Figure 1. Five different models were used to assess the influence of solvent. The vacuum is not signified, whereas the solvent models are indicated by a two-letter code to reflect the single- (1W), two- (2W), and three-water (3W) explicit models; the PCM (P0) continuum model; and the combined discrete-continuum strategy of two waters with PCM (P2). For example, the *endo s-cis* acrolein transition structure studied by the two-water explicit model with the B3LYP/6-31G(d) level of theory is indicated as NC2W.

Activation Energies. The calculated absolute energies and thermodynamic corrections from frequency analyses at 298.15 K and 1 atm for acrolein, butadiene, and transition structures are given in the Supporting Information. The computed activation energies, enthalpies, and Gibbs energies in a vacuum and water approximated environments are presented in Table 1. In the case of one- and two-water explicit models, the activation energies are computed by subtracting the isolated butadiene and the hydrogen-bonded acrolein and water-complex energies from the total transition structure energy. The explicit three-water computation with acrolein is problematic. The third water minimizes to interact with the other waters and not acrolein. It is important to retain similar water positions around acrolein so that the stabilization energies reflect the specific interaction differences between the transition structure and the ground state. To circumvent the problem, the activation energy is computed by subtracting the isolated butadiene, the hydrogen-bonded two-water acrolein complex, and the third isolated water energies from the total transition structure energy. Consequently, the lowering of the activation for the three-water explicit model is

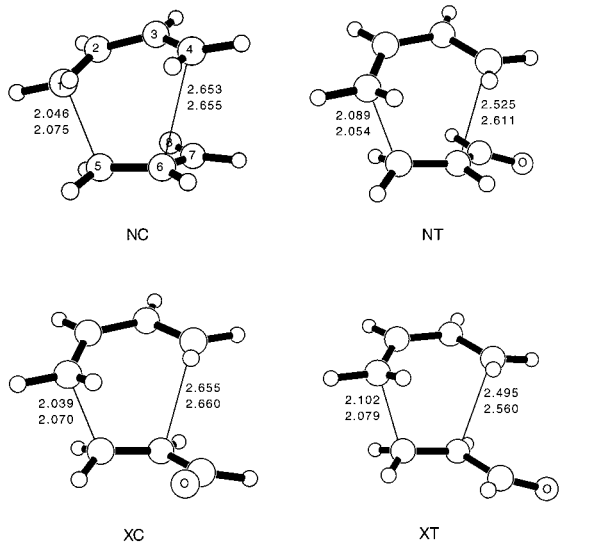

Figure 1. Transition structures of the reaction between butadiene and acrolein in the gas phase. Bond lengths (Å) are given for vacuum (top), and solvent (PCM).

Table 1. Activation Energies, Enthalpies, and Gibbs Energies (kcal/mol) of the Reaction between 1,3-Butadiene and Acrolein in Vacuum, PCM, and Explicit Water[a]

TS	$\Delta E^{\ddagger}_0$[b]	$\Delta E^{\ddagger}_{298}$	$\Delta H^{\ddagger}_{298}$	$\Delta G^{\ddagger}_{298}$
		Vacuum		
NC	20.1	19.6	19.1	32.2
NT	21.4	20.9	20.3	33.5
XC	20.2	19.7	19.2	32.2
XT	22.0	21.6	21.0	34.1
		PCM (P0)[c]		
NCP0	16.4	15.9	15.3	28.9
NTP0	17.1	16.6	16.0	29.6
XCP0	17.5	17.0	16.4	30.0
XTP0	18.3	17.7	17.1	31.0
		One Water (1W)		
NC1W	17.4	16.9	16.3	30.0
NT1W	19.3	18.9	18.3	31.5
XC1W	17.7	17.2	16.6	30.5
XT1W	20.0	19.6	19.0	32.1
		Two Water (2W)		
NC2W	16.0	15.5	14.9	28.8
NT2W	18.1	17.8	17.2	30.3
XC2W	17.1	16.6	16.0	29.7
XT2W	18.9	18.5	17.9	31.2
		Three Water (3W)		
NC3W	13.8	14.3	13.1	32.5

[a] Using the B3LYP/6-31G(d) level of theory. [b] Zero-point energy included. [c] The dielectric constant of water, 78.39, was used.

(101) Kistiakowaki, G. B.; Lacher, J. R. *J. Am. Chem. Soc.* **1936**, *58*, 123.
(102) Blankenburg, V. B.; Fiedler, H.; Hampel, M.; Hauthal, H. G.; Just, G.; Kahlert, K.; Korn, J.; Müller, K.-H.; Pritzkow, W.; Reinhold, Y.; Röllig, M.; Sauer, E.; Schnurpfeil, D.; Zimmermann, G. *J. Prakt. Chem.* **1974**, *316*, 804.
(103) Mulliken, R. S. *J. Chem. Phys.* **1955**, *23*, 1833.
(104) Davidson, E. R. *J. Chem. Phys.* **1967**, *46*, 3320.
(105) Singleton, D. A. *J. Am. Chem. Soc.* **1992**, *114*, 6563.
(106) Birney, D. M.; Houk, K. N. *J. Am. Chem. Soc.* **1990**, *112*, 4127.
(107) Alston, P. V.; Ottenbrite, R. M.; Cohen, T. *J. Org. Chem.* **1978**, *43*, 1864.
(108) Salem, L. *J. Am. Chem. Soc.* **1968**, *90*, 553.
(109) Breneman, C. M.; Wiberg, K. B. *J. Comput. Chem.* **1990**, *11*, 361.
(110) Cox, S. R.; Williams, D. E. *J. Comput. Chem.* **1981**, *2*, 304.
(111) Chirlian, L. E.; Francl, M. M. *J. Comput. Chem.* **1987**, *8*, 894.
(112) Carlson, H. A.; Nguyen, T. B.; Orozco, M.; Jorgensen, W. L. *J. Comput. Chem.* **1993**, *14*, 1240.

Table 2. Activation Energies, Enthalpies, and Gibbs Energies (kcal/mol) of the Reaction between 1,3-Butadiene and Acrolein[a]

TS	$\Delta E^{\ddagger}_0$[b]	$\Delta E^{\ddagger}_{298}$	$\Delta H^{\ddagger}_{298}$	$\Delta G^{\ddagger}_{298}$
		Benzene		
NCP0	18.7	18.2	17.6	30.9
NTP0	19.9	19.4	18.8	32.1
XCP0	19.1	18.7	18.1	31.1
XTP0	20.6	20.2	19.6	32.6
		Methylene Chloride		
NCP0	18.7	18.1	17.6	31.0
NTP0	19.3	18.9	18.3	31.4
XCP0	19.1	18.7	18.1	31.2
XTP0	20.4	19.9	19.3	32.4
		Methanol		
NCP0	17.5	17.1	16.5	30.0
NTP0	18.2	17.7	17.2	30.8
XCP0	18.3	17.9	17.3	30.5
XTP0	19.2	18.8	18.2	31.6

[a] Computed using PCM and the B3LYP/6-31G(d) level of theory in different solvents [b] Zero-point energy included.

overestimated (by ca. 1 kcal/mol), because the ground state does not benefit from the third water interaction. For the continuum method, the activation energies are determined by subtracting each of the isolated component energies from the total transition structure energy.

The computed activation energy of 19.6 kcal/mol in a vacuum at 298 K is in excellent agreement with the experimental value of 19.7 kcal/mol.[101] In toluene, the experimental activation enthalpy is 15.8 ± 1.4 kcal/mol, with an activation entropy of −38 ± 4 cal/mol-K.[102] Therefore, the computed 19.1 kcal/mol gas-phase activation enthalpy of acrolein and butadiene should be lowered by 3.3 kcal/mol in toluene. In a related Diels−Alder reaction of cyclopentadiene and methyl acrylate, the experimental activation enthalpy is 15.1 kcal/mol in toluene, which is ca. 0.7 kcal/mol lower than that reported for acrolein and butadiene.[53] In addition, the activation enthalpy and entropy for the cyclopentadiene and methyl acrylate reaction is 10.2 kcal/mol and −40.9 cal/mol-K, respectively, in a methanol/water mixture.[53] Therefore, analogous to the cyclopentadiene and methyl acrylate reaction, the butadiene and acrolein activation enthalpy (adjusted by 0.7 kcal/mol) is expected to be ca. 10.9 kcal/mol in a methanol/water mixture, which is 8.2 kcal/mol lower than the 19.1 kcal/mol gas-phase activation enthalpy.

An activation enthalpy lowering with increasing solvent polarity is provided by the PCM method, as shown in Tables 1 and 2. The gas-phase NC activation enthalpies decrease by 1.5, 1.5, 2.6, and 3.8 kcal/mol in benzene, methylene chloride, methanol, and water, respectively. In benzene (dielectric similar to toluene), the computed activation enthalpy is 17.6, or 1.5 kcal/mol lower than the gas-phase activation enthalpy. As compared to the experimental observation of 15.8 ± 1.4 kcal/mol in toluene,[102] the PCM method recovers ca. 45% (1.5 kcal/mol computed per 3.3 kcal/mol expected) of the experimental solvation effect. In aqueous solution, the PCM method computes an activation enthalpy of 15.3 kcal/mol, which is 46% (3.8 kcal/mol computed per 8.2 kcal/mol expected) of the estimated reduction to a 10.9 kcal/mol activation barrier. In a second comparison, the second-order rate constants between cyclopentadiene and alkyl vinyl ketones have been reported to be 740 times larger in water than in *n*-octane.[66] Overall, the PCM model lowers the Gibbs activation energies of the NC reaction from benzene to water by 2.0 kcal/mol, which corresponds to an aqueous rate increase of ca. 30 times. Therefore, despite mirroring the experimental trend in activation barrier reduction with increasing solvent polarity, the PCM method does not fully account for the observed rate of aqueous acceleration.

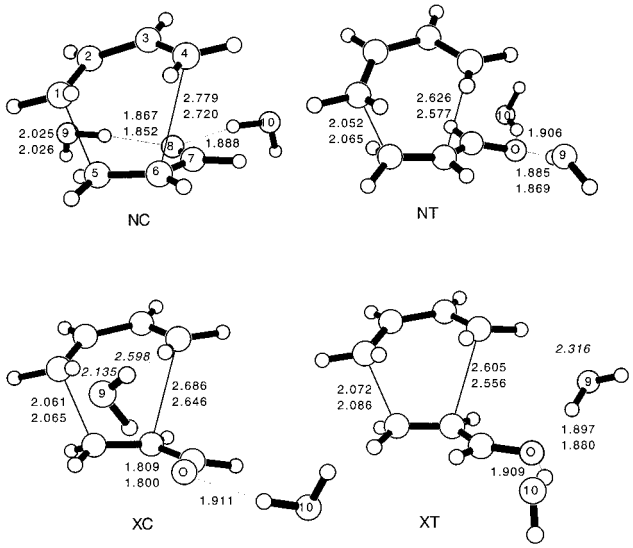

Figure 2. Transition structures of the reaction between butadiene and acrolein with two explicit water molecules. Bond lengths (Å) are given for two explicit waters (top), and one explicit water (bottom). Distances (Å) are shown for interactions of the water molecule in the two-explicit-water model and butadiene hydrogens (italics).

Compared to a vacuum, one explicit water lowers the activation barrier of the NC pathway by 2.8 kcal/mol. With two explicit waters (see Figure 2), the activation enthalpy is lowered by 4.2 kcal/mol. Thus, the single-water model picks up 70% of the two-water model activation barrier lowering. In the two-water explicit model, an activation enthalpy of 14.9 kcal/mol is computed, which is 51% (4.2 kcal/mol computed per 8.2 kcal/mol expected) of the estimated activation barrier reduction to 10.9 kcal/mol. An induced charge separation across the dienophile double bond suggests that a third explicit water could possibly cause significant stabilization of the transition structure. As shown below, the CHELPG charges are given from the vacuum (top) and explicit two-water model (bottom).

Scheme 1. Atomic Charges in the NC Transition Structure Given from the Vacuum (top) and Explicit Two-Water Model (bottom)

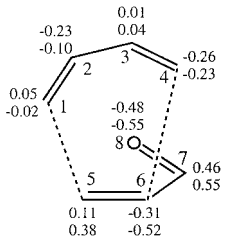

The enhanced charge distribution, particularly the increased positive charge on the C_2 of the diene, and the negative charge build-up on C_6 and O_8 of the dienophile fragments are consistent with earlier comparisons of the charges from the allyl cation with butadiene and the enolate anion with acrolein.[106] The transition structure with three waters is shown in Figure 3. The third water is attracted to the induced charge separation across the dienophile double bond. The computed NC3W activation enthalpy is 13.1 kcal/mol, or 1.8 kcal/mol lower than that computed for NC2W. The explicit three water model recovers 73% (6 kcal/mol computed per 8.2 kcal/mol expected) of the expected lowering of the activation energy. The procedure for computing the NC3W activation energy makes the 13.1 kcal/

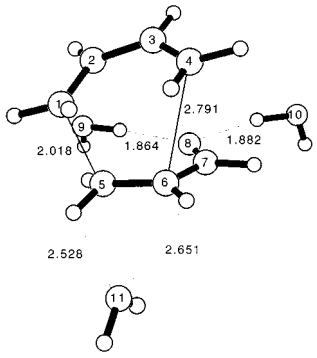

Figure 3. Transition structures of the reaction between butadiene and acrolein with three explicit waters. Units in Å.

Table 3. Single Point $\Delta E^{\ddagger}_0$[a] Activation Energies (kcal/mol) of the Reaction between 1,3-Butadiene and Acrolein[b]

	PCM, two water (P2)	
TS	methanol	water
NCP2	11.5	12.3
NTP2	16.1	13.2
XCP2	13.7	14.7
XTP2	13.2	13.9

[a] Zero point energy not included. [b] Using PCM and two explicit waters at the B3LYP/6-31G(d) level of theory.

mol an overestimation, as discussed earlier. An activation of approximately 14.1 kcal/mol (ca. 1 kcal/mol greater) is more realistic. Thus, only 10% more of the activation energy lowering is recovered, as compared to NC2W. In the absence of including all of the water explicitly, the computations indicate that the explicit two-water model represents a majority of the possible local microscopic phenomena through hydrogen bonding. Consequently, both the implicit and discrete models account for approximately one-half of the observed rate acceleration caused by the aqueous phase.

The PCM and discrete water models are fundamentally different in the description of solvation effects.[96] The question arises whether the PCM and discrete water models account for the same portion of the observed acceleration. Thus, a combined discrete-continuum (P2) strategy using both PCM and explicit waters was employed. Full transition structure searches using PCM and two explicit waters proved to be problematic, because stationary points could not be located. Thus, single point energy evaluations were carried out on the two-water transition structures using PCM. The results are given in Table 3. To simulate the methanol/water mixture, P2 single point energy evaluations in methanol were also carried out. Because single point evaluations are not thermally corrected, the expected activation enthalpy lowering of 8.2 kcal/mol must be adjusted. The average difference between computed $\Delta E^{\ddagger}_0$ and $\Delta H^{\ddagger}_{298}$ values in Table 1 is 1.0 ± 0.2 kcal/mol, which is relatively constant. Therefore, the expected aqueous-phase activation energy for the acrolein and butadiene reaction is assumed to be 1 kcal/mol greater than the expected activation enthalpy (8.2 kcal/mol), or 9.2 kcal/mol. The P2 computed NC activation energy lowering of $20.1 - 12.3 = 7.8$ kcal/mol (water) and $20.1 - 11.5 = 8.6$ kcal/mol (methanol/water) recovers 85% and 93% of the expected 9.2 kcal/mol activation energy reduction, respectively.[53] The results indicate that the catalytic effect of water manifests itself by a combination of both bulk and local microsolvation phenomena.

To better understand bulk-phase effects, the computed activation energy lowering in a methanol/water mixture, as compared to pure water, was examined. PCM single point evaluations on the two-water transition structure (P2 method) produced solvent-corrected activation energies of 12.3 (water) and 11.5 kcal/mol (methanol/water), as shown in Table 3. The computed activation lowering in the water/methanol mixture is consistent with the idea of antihydrophobic effects.[70−73] Essentially, the dielectric of the cavity provided by the continuum interacts with the induced charge polarization of the transition structure caused by the two explicit waters. Hydrophobic regions of the transition structure are better stabilized by the lower dielectric (methanol) provided by the continuum cavity. The magnitude of the antihydrophobic effect is estimated to be the induced energetic preference of the methanol/water mixture over pure water ($12.3-11.5 = 0.8$ kcal/mol), based upon the P2 computations listed in Table 3, plus the energy to destabilize pure water over methanol ($17.5 - 16.4 = 1.1$ kcal/mol) by the P0 computations in Tables 1 and 2. Consequently, 1.9 kcal/mol of the bulk-phase effect is composed of an antihydrophobic interaction, which accounts for ca. 21% (1.9 kcal/mol computed per 9.2 kcal/mol expected) of the activation energy lowering. The remaining $4.6 - 1.9 = 2.7$ kcal/mol or 29% (2.7 kcal/mol remaining per 9.2 kcal/mol expected) is attributed to the enforced hydrophobic effect. The computed 2.7 kcal/mol effect is slightly greater than the simulation work by Jorgensen[54,63] and smaller than the QM/MM value reported by Gao.[61] A few significant results should be mentioned. First, it is necessary to induce the charge polarization of the NC transition structure by explicit hydrogen bonds in order to generate the bulk phase effects. Comparison of the activation enthalpies between P0 and P2 continuum models illustrates the effect of explicit hydrogen bonding. Second, local hydrogen bonding accounts for a large portion of the rate enhancement (50%), and the bulk phase composed of enhanced hydrophobic interactions (30%) and antihydrophobic effects (20%) describe the remainder of the rate acceleration observed by experiment.

Transition Structures Geometries. Unsymmetrical dienophiles, such as acrolein, produce concerted and asynchronous transition structures, as computed by semiempirical,[48−52] Hartree−Fock,[13,14,53−55,106,113−115] MCSCF,[116,117] Møller−Plesset,[59,118] and density functional theory.[56−58,119] Shown in Figure 1 are the four gas-phase transition structures computed at the B3LYP/6-31G(d) level of theory. The geometries of the noncatalyzed reaction are the same as those previously reported by García and co-workers.[56] The geometry-optimized PCM structures are also included in Figure 1. The four transition structures computed using the two-water discrete model with B3LYP/6-31G(d) are shown separately in Figure 2. The geometries from the one-water discrete model are also indicated in the figure. The three-water explicit model for the NC transition structure is given in Figure 3. The critical geometric parameters from the vacuum and water models are summarized in Table 4, and the geometries from different PCM solvent computations are given in Table 5. The degree of asynchronicity promoted by solvent effects is measured by the difference in the breaking/

(113) Imade, M.; Hirao, H.; Omoto, K.; Fujimoto, H. *J. Org. Chem.* **1999**, *64*, 6697, and references therein.
(114) Domingo, L. R.; Picher, M. T.; Andrés, J.; Safont, V. S. *J. Org. Chem.* **1997**, *62*, 1775.
(115) Suárez, D.; Sordo, T. L.; Sordo, J. A. *J. Am. Chem. Soc.* **1994**, *116*, 763.
(116) Storer, J. W.; Raimondi, L.; Houk, K. N. *J. Am. Chem. Soc.* **1994**, *118*, 9675.
(117) Bernardi, F.; Bottoni, A.; Field, M. J.; Guest, M. F.; Hillier, I. H.; Robb, M. A.; Venturini, A. *J. Am. Chem. Soc.* **1988**, *110*, 3050.
(118) Suárez, D.; Sordo, J. A. *J. Chem. Soc., Chem. Commun.* **1998**, 385.
(119) Singleton, D. A.; Merrigan, S. R.; Beno, B. R.; Houk, K. N. *Tetrahedron Lett.* **1999**, *40*, 5817.

Table 4. Key Distances (Å) of the 1,3-Butadiene and Acrolein Transition Structure Computed at the B3LYP/6-31G(d) Level of Theory in Vacuum, PCM, and Explicit Water

TS	NC	NT	XC	XT
		Vacuum		
1-5	2.046	2.089	2.039	2.102
4-6	2.653	2.525	2.655	2.495
4-7	2.918	2.850	2.974	2.943
3-7	3.069	3.296	3.885	3.915
2-8	3.316	4.899	4.475	5.224
		PCM (P0)[a]		
1-5	2.075	2.054	2.070	2.079
4-6	2.655	2.611	2.660	2.560
4-7	2.857	2.839	2.968	3.007
3-7	3.083	3.288	3.874	3.933
2-8	3.454	4.879	4.574	5.235
		Two Water (2W)		
1-5	2.025	2.052	2.061	2.072
4-6	2.779	2.626	2.686	2.605
4-7	2.917	2.848	2.968	3.008
3-7	3.083	3.299	3.856	3.910
2-8	3.347	4.856	4.775	5.152

[a] The dielectric constant of water, 78.39, was used.

Table 5. Key Distances (Å) of the 1,3-Butadiene and Acrolein Transition Structure Computed with PCM and the B3LYP/6-31G(d) Level of Theory in Different Solvents

TS	NC	NT	XC	XT
		Benzene		
1-5	2.048	2.092	2.051	2.105
4-6	2.687	2.540	2.665	2.508
4-7	2.903	2.835	2.962	2.941
3-7	3.029	3.283	3.865	3.905
2-8	3.234	4.892	4.456	5.220
		Methylene Chloride		
1-5	2.056	2.079	2.054	2.093
4-6	2.673	2.565	2.668	2.531
4-7	2.892	2.842	2.959	2.955
3-7	3.053	3.292	3.864	3.906
2-8	3.320	4.898	4.503	5.218
		Methanol		
1-5	2.071	2.052	2.064	2.065
4-6	2.655	2.610	2.661	2.575
4-7	2.863	2.847	2.978	3.016
3-7	3.093	3.295	3.883	3.938
2-8	3.471	4.885	4.579	5.229

forming bond distances, $\Delta d = (C_4C_6 - C_1C_5)$, and by the pyramidalization[120] of the four reacting carbon centers, that is, $\Delta p_5 = (\angle C_6C_5HH - 180°)$, as summarized in the Supporting Information.

Gas-Phase Asynchronicity. Asynchronicity of the Diels−Alder reaction for unsymmetrical dienophiles has been reported previously by theory[13] and experiment.[119,121−123] As a first step to understanding solvent effects on the rates of Diels−Alder reactions, the degree of transition structure asynchronicity is measured in the gas phase. As discussed by Birney and Houk, frontier molecular orbital (FMO) theory can be used to rationalize the asynchronicity of Diels−Alder transition structures.[106] Briefly, the acrolein LUMO has a large coefficient on the β carbon (C_5 in this case), which makes it more electrophilic than the α carbon (C_6). Consequently, greater overlap between the β carbon and the diene HOMO leads to a stronger and shorter C_1C_5 bond at the transition structure. Indeed, the computations produce an *s-cis* acrolein LUMO β coefficient (0.81) nearly twice as large as that of the α carbon (−0.47). From the gas-phase analysis, the *s-trans* transition structures ($\Delta d^{NT} = 0.44$ Å and $\Delta d^{XT} = 0.39$ Å) are computed to be more synchronous than the corresponding *s-cis* structures ($\Delta d^{NC} = 0.61$ Å and $\Delta d^{XC} = 0.62$ Å). The computed LUMO carbon coefficient differences (*s-trans* LUMO $\beta = 0.82$ and *s-trans* LUMO $\alpha = -0.49$) do not justify the large asynchronicity change between the *s-trans* and *s-cis* transition structures. As discussed later, subtle electronic and steric transition structure interactions are found to perturb the flexible stationary points. Despite the enhanced asynchronicity, extensive searches have not produced lower energy intermediates that would indicate a change from a concerted mechanism.

As compared to the synchronous parent ethene and butadiene Diels−Alder transition structure with breaking/forming bonds of 2.272 Å ($\Delta d = 0$ Å) computed with B3LYP/6-31G(d), the acrolein and butadiene NC transition structure C_1C_5 bond is shorter by 0.23 Å and the C_4C_6 bond is longer by 0.38 Å. The increased pyramidalization of the reacting centers C_1 (8°) and C_5 (11°) and the reduced pyramidalization of C_4 (−13°) and C_6 (−17°) are consistent with a greater transition structure asynchronicity when replacing ethene with acrolein as the dienophile. As compared to the synchronous ethene and butadiene reaction, the four computed gas-phase transition structures have breaking/forming bonds 0.17−0.23 Å shorter for the C_1C_5 bond and 0.22−0.38 Å longer for the C_4C_6 bond. In addition, the C_1, C_4, C_5, and C_6 pyramidalizations differ by 6−8°, −9 to −13°, 9−11°, and −7 to −17°, respectively. The C_4 and C_6 centers have more variance, consistent with Houk's ideas concerning transition state flexibility.[106] Therefore, when replacing ethene with acrolein as the dienophile, significant geometric changes occur, yet the differences among the four stereospecific transition structures are more narrowly defined.

The importance of electron correlation in geometry optimizations is illustrated by contrasting the density functional results against previous Hartree−Fock calculations with the 3-21G basis set for the acrolein and butadiene reaction.[56,59,106] The HF/3-21G breaking/forming C_1C_5 and C_4C_6 bond lengths in the NC reaction are 2.088 and 2.353 Å ($\Delta d^{NC} = 0.27$ Å), and the pyramidalization of C_1, C_4, C_5, and C_6 are only 11, 2, 11, and 3°, respectively.[106] Therefore, the Hartree−Fock transition structure is significantly more synchronous, with $\Delta\Delta d^{HF-DFT} = -0.34$ Å, and the reactive centers more planar ($\Delta\Delta p_1 = -22°$ and $\Delta\Delta p_5 = -24°$) as compared to the B3LYP/6-31G(d) structure. Because the importance of electron correlation in Diels−Alder mechanistic issues has been documented recently,[56,59] it is assumed that the more asynchronous B3LYP/6-31G(d) transition structure is a more appropriate starting point in approximating the effect of solvent.

Solution Phase Asynchronicity. PCM geometry optimizations predict a slight decrease in the *s-cis* ($\Delta\Delta d^{NC} = -0.03$ Å and $\Delta\Delta d^{XC} = -0.02$ Å) and a small increase in the *s-trans* ($\Delta\Delta d^{NT} = 0.12$ Å and $\Delta\Delta d^{XT} = 0.09$ Å) transition structure asynchronicities from the gas to aqueous phase. The explicit solvation model produces more significant geometric changes on the transition structures. The two-water transition structures are shown in Figure 2. The waters energy minimize to hydrogen bonding positions with the carbonyl lone pairs of acrolein. In the two-water explicit model, each transition structure has increased asynchronicity. The *s-trans* asynchronicity increases from $\Delta d^{XT} = 0.39$ to 0.53 Å and from $\Delta d^{NT} = 0.44$ to 0.57 Å from vacuum to water. The *s-cis* asynchronicity increases from

(120) Haddon, R. C. *Acc. Chem. Res.* **1988**, *21*, 243.
(121) Telan, L. A.; Firestone, R. A. *Tetrahedron* **1999**, *55*, 14269.
(122) Gajewski, J. J.; Peterson, K. B.; Kagel, J. R. *J. Am. Chem. Soc.* **1987**, *109*, 5545.
(123) Tolbert, L. A.; Ali, B. *J. Am. Chem. Soc.* **1984**, *106*, 3806.

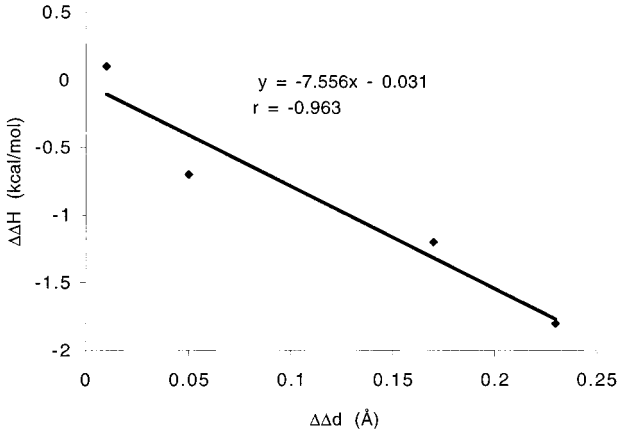

Figure 4. Activation enthalpy differences versus asynchronicity in a vacuum.

$\Delta d^{NC} = 0.61$ to 0.75 Å and from $\Delta d^{XC} = 0.62$ to 0.63 Å. In the NC2W transition structure, the C_1C_5 bond decreases to 2.025 Å, and the C_4C_6 bond increases to 2.779 Å ($\Delta d^{NC2W} = 0.75$ Å). The change of pyramidalization of the reactive carbons is less than 5°. Therefore, the preferred NC2W transition structure is more asynchronous in water ($\Delta\Delta d^{NC2W-NC} = 0.14$ Å). Smaller asynchronicity changes were induced in XC2W. The pyramidalization change for the reactive centers is less than 2°. Thus, the explicit two-water model produces a magnified asynchronicity difference between the NC and XC transition structures in water which was not predicted by the PCM method.

It is generally accepted that asynchronicity increases in Diels−Alder transition structures result in a corresponding activation energy barrier lowering.[55,124] Recently, this general and empirical guideline has been questioned.[56] As described previously, the vacuum *s-trans* transition structures ($\Delta d^{NT} = 0.44$ Å and $\Delta d^{XT} = 0.39$ Å) are computed to be more synchronous than the corresponding *s-cis* structures ($\Delta d^{NC} = 0.61$ Å and $\Delta d^{XC} = 0.62$ Å). Consistent with the hypothesis, NT is 1.2 kcal/mol greater in energy than NC, XT is 1.8 kcal/mol greater than XC, and XT is 0.7 greater than NT. Even when comparing NC and XC in the gas phase, the asynchronicities ($\Delta\Delta d^{NC-XC} = -0.01$ Å) and activation barriers ($\Delta\Delta H^{NC-XC} = -0.1$ kcal/mol) are essentially the same within the accuracy of the computations. In this study, the gas-phase results follow the general guidelines. In fact, a strong relationship between gas-phase activation enthalpy and asynchronicity is computed and plotted in Figure 4. The resulting correlation coefficient is −0.96 in a vacuum.

In water, the *s-trans* asynchronicities are $\Delta d^{NT} = 0.56$ (P0) and 0.57 Å (2W), and $\Delta d^{XT} = 0.48$ (P0) and 0.53 Å (2W). The *s-cis* asynchronicities are $\Delta d^{NC} = 0.58$ (P0) and 0.75 Å (2W), and $\Delta d^{XC} = 0.59$ (P0) and 0.63 Å (2W). NT2W is 2.3 kcal/mol greater in energy than NC2W, XT2W is 1.9 kcal/mol greater than XC2W, XT2W is 0.7 kcal/mol greater than NT2W, and XC2W is 1.1 kcal/mol greater than NC2W. Even though the trend holds between asynchronicity and energy differences in solution, the correlation is not so strong as in a vacuum. The resulting correlation coefficient in the explicit two-water model is 0.82. A closer examination of the data shows that the synchronicity differences between a vacuum and water ($\Delta\Delta d^{NT} = 0.13$ Å, $\Delta\Delta d^{XT} = 0.14$ Å, $\Delta\Delta d^{NC} = 0.14$ Å, and $\Delta\Delta d^{XC} = 0.01$ Å) are constant, except for the XC transition structure. As shown in Figure 2, the XC transition structure provides the only opportunity for the explicit waters to bridge with the hydrogens from butadiene. The importance of other external interactions have been described recently.[125] It is this bridging water interaction that maintains the XC vacuum asynchronicity and skews the linear relationship between asynchronicity and enthalpy lowering of the four stereospecific transition structures. Due to the small asynchronicity changes computed by PCM, no correlation could be identified.

Scheme 2. Possible Secondary Orbital Overlap Interactions[a]

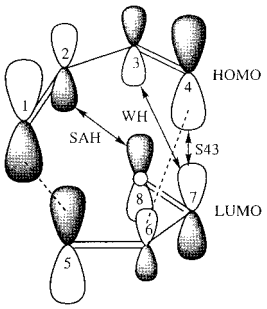

[a] Abbreviated are the Salem, Alston and Houk (SAH), Woodward and Hoffmann (WH), and Singleton [4+3] (S43) interactions.

Endo/Exo Selectivity. Frontier molecular orbital (FMO) theory[108,126,127] and the Woodward−Hoffmann rules[128] provide a theoretical framework to analyze the unusual reactivity, selectivity, and asynchronicity of Diels−Alder reactions. Initially, Alder created the rule of "maximum accumulation of unsaturation" to explain the stereospecificity and *endo* selectivity of Diels−Alder reactions.[129] Subsequently, Woodward and Hoffmann,[128] Houk,[130] Salem,[108] Alston,[107] and Singleton[105] proposed specific secondary orbital interactions to rationalize the preference of *endo* cycloadditions. Interpretations based upon secondary orbital interactions are known to be controversial.[106,118] Therefore, alternative explanations for *endo* selectivity based on inductive,[131−133] dipole−dipole,[134] charge-transfer,[135] electrostatic,[136] and steric interactions[15] have been reported. Briefly, secondary orbital interactions are the transition structure terms that do not involve covalent bond making or breaking. From FMO theory, the diene HOMO and dienophile LUMO coefficients allow for a number of positive overlaps, or stabilizing interactions, in which three of the individual secondary orbital interactions are considered and illustrated in Scheme 2. The classical secondary orbital interactions defined by Woodward and Hoffmann resulted from the FMO treatment of butadiene dimerization.[128] Because the ground-state LUMO coefficient on the carbonyl carbon (C_7) of acrolein is relatively large, a great amount of experimental and theoretical effort has been invested in this classical C_3C_7 Woodward and Hoffmann interaction,[50,51,137−139] which is labeled as WH in the Scheme.

(124) Froese, R. D. J.; Organ, M. G.; Goddard, J. D.; Stack, T. D. P.; Trost, B. M. *J. Am. Chem. Soc.* **1995**, *117*, 10931.
(125) Sodupe, M.; Rios, R.; Branchadell, B.; Nicholas, T.; Oliva, A.; Dannenberg, J. J. *J. Am. Chem. Soc.* **1997**, *119*, 4232.
(126) Fukui, K. *Acc. Chem. Res.* **1971**, *4*, 57.
(127) Salem, L. *J. Am. Chem. Soc.* **1968**, *90*, 543.
(128) Woodward, R. B.; Hoffmann, R. *The Conservation of Orbital Symmetry*; Verlag Chemie: Weinheim, 1970.
(129) Alder, K. *Annalen* **1951**, *571*, 87.
(130) Houk, K. N. *Tetrahedron Lett.* **1970**, 2621.
(131) Wassermann, A. *J. Chem. Soc.* **1935**, 828.
(132) Wassermann, A. *J. Chem. Soc.* **1935**, 1511.
(133) Wassermann, A. *J. Chem. Soc.* **1936**, 432.
(134) Berson, J. A.; Hamlet, Z.; Mueller, W. A. *J. Am. Chem. Soc.* **1962**, *84*, 297.
(135) Woodward, R. B.; Baer, H. *J. Am. Chem. Soc.* **1944**, *66*, 645.
(136) Kahn, S. D.; Pau, C. F.; Overman, L. E.; Hehre, W. J. *J. Am. Chem. Soc.* **1986**, *108*, 7381.
(137) Ginsburg, D. *Tetrahedron* **1983**, *39*, 2095.
(138) Fox, M. A.; Cardona, R.; Kiweit, N. J. *J. Org. Chem.* **1987**, *52*, 1469.
(139) Apeloig, Y.; Matzner, E. *J. Am. Chem. Soc.* **1995**, *117*, 5375.

Table 6. Mulliken Overlap of the 1,3-Butadiene and Acrolein Transition Structure Computed at the B3LYP/6-31G(d) Level of Theory in Vacuum, PCM (P0), Explicit Water (2W), and the Combination of PCM and Explicit Water (P2)

TS	NC	NT	XC	XT
		Vacuum		
3-7 (WH)	0.0018	−0.0015	−0.0000	0.0005
4-7 (S43)	0.0030	0.0060	0.0018	0.0019
2-8 (SAH)	0.0094	0.0000	0.0002	0.0000
total components	0.0142	0.0045	0.0020	0.0024
total	0.0187		0.0044	
		PCM (P0)[a]		
3-7 (WH)	0.0026	−0.0014	−0.0002	0.0003
4-7 (S43)	0.0059	0.0103	0.0036	0.0046
2-8 (SAH)	0.0065	0.0000	0.0001	0.0000
total components	0.0150	0.0089	0.0035	0.0049
total	0.0239		0.0084	
		Two Water (2W)		
3-7 (WH)	0.0019	−0.0013	−0.0004	−0.0000
4-7 (S43)	0.0088	0.0140	0.0087	0.0063
2-8 (SAH)	0.0069	0.0001	0.0001	0.0000
total components	0.0177	0.0128	0.0084	0.0063
total	0.0305		0.0147	
		PCM, two water (P2)		
3-7 (WH)	0.0023	−0.0016	−0.0005	−0.0001
4-7 (S43)	0.0110	0.0165	0.0097	0.0073
2-8 (SAH)	0.0069	0.0000	0.0001	0.0000
total components	0.0202	0.0149	0.0093	0.0072
total	0.0351		0.0165	

[a] The dielectric constant of water, 78.39, was used.

Independent theoretical studies of the butadiene and acrolein reaction by Salem,[108] Houk,[130] and Alston,[107] found little evidence to support the classical WH secondary orbital interaction. Instead, positive Mulliken overlap population between the C_2 atom of butadiene and the oxygen (O_8) of acrolein indicated a more important interaction, as given by SAH in the Scheme. Finally, Singleton reported that secondary orbital interactions involving bond-making/-breaking centers are possible.[105] On the basis of Mulliken overlap populations and geometric distortions, a new secondary orbital interaction, also called the [4+3] interaction, between the C_4 atom of butadiene and the carbonyl carbon (C_7) of acrolein has been determined,[105] which is denoted by S43 in the Scheme.

The gas-phase *s-trans* transition structure is computed to be more *endo*-selective than the *s-cis* transition structures for acrolein and butadiene[56] and other Diels−Alder reactions.[53,54,140] Consistent with experimental trends,[113] the calculated gas-phase *endo* selectivities, based upon the activation enthalpies, are 0.1 kcal/mol (*s-cis*) and 0.7 kcal/mol (*s-trans*). Enhanced *endo/exo* selectivity also has been observed in aqueous solvents experimentally,[10,67,68,90] which has been explained by solvent solvophobicity[85−90] and hydrogen bonding.[22−26,28,54,55,62] The calculated enhancement of *endo* selectivity for the *s-cis* transition structures increases to 1.1 (P0), 1.1 (2W), and 2.4 kcal/mol (P2), whereas the *s-trans endo* selectivity results in 1.1 (P0), 0.7 (2W), and 0.7 kcal/mol (P2) in water. Thus, the *endo* selectivity increases substantially for the *s-cis* structures when treated by the discrete-continuum method in the aqueous phase, while the *s-trans* remains relatively immune to solvent changes. The discrete-continuum computations deliver the observed gas- and aqueous-phase *endo* selectivity, as reported by experiment.

The Mulliken overlap populations from the density functional computations are given in Table 6. In a vacuum, it is clear that all three secondary orbital interactions contribute to the NC enhanced stability. Consistent with previous reports,[108,130] the SAH term is found to dominate the secondary orbital interactions (0.009), as compared to S43 (0.003) and WH (0.002). Summed together, the total secondary overlap from the gas-phase Mulliken population is 0.014 for NC. For each of the other transition structures, the Mulliken overlap terms become insignificant or repulsive, except for the S43 interaction. The XC, NT, and XT transition structures have 0.002, 0.005, and 0.002 S43 Mulliken population overlaps, respectively, which are roughly an order of magnitude less than the combined terms of NC. Consequently, all three possible secondary orbital interactions contribute to the total Mulliken population overlap of the NC transition structure, although only the S43 impacts the other transition structures. Therefore, this explanation of *endo* selectivity is consistent with the original rule[129] of "maximum accumulation of unsaturation."

When the effect of water is included by PCM, the discrete two-water model, or the discrete-continuum P2 model, the contributions from the different terms become modified significantly. As in the vacuum, all three secondary orbital interactions contribute to the NC transition structure. The Mulliken overlap term for WH remains steady at ca. 0.002, SAH declines slightly to 0.007, and Singleton's S43 term increases to a maximum of 0.011 when the P2 method is used, as compared to a vacuum. The accumulation of overlap populations in water is 0.015 (P0), 0.018 (2W), and 0.020 (P2). As is found in the vacuum, the Mulliken populations for all terms except S43 either are reduced to zero or become repulsive for the three other transition structures. Singleton's S43 term increases dramatically in strength, which is a maximum for the P2 model. The summed Mulliken population overlap contributions are 0.020 for NC, 0.009 for XC, 0.015 for NT, and 0.007 for XT when using the P2 model.

To compare the *endo/exo* selectivity, NC and NT are added to give an *endo* Mulliken population overlap of 0.0187 (vacuum), with an *exo* Mulliken population of 0.0044 (vacuum). Direct comparison to the solvation models show that *endo/exo* Mulliken population overlaps of 0.0239/0.0084 (P0), 0.0305/0.0147 (2W), and 0.0351/0.0165 (P2) result. The *endo/exo* selectivity is gauged by the Mulliken population difference, in which in a vacuum the overlap is 0.014 greater for the *endo* transition structure. Consistent with the interpretation that the catalytic effect of water manifests itself by both bulk and local microsolvation phenomena, we find that the increase in *endo* selectivity is increased equally, to 0.016, by both bulk effects (P0) and explicit hydrogen bonding (2W). The discrete-continuum method delivers the combination of both effects, in which the Mulliken population difference increases to 0.019. Therefore, an enhanced *endo* selectivity in the aqueous phase is computed over a vacuum, where ca. 50% of the effect is delivered by enhanced hydrogen bonding (discrete computations) and the remainder by bulk phase effects (continuum methods). Again, the results are consistent with the accumulation of maximum overlap, because it is the sum of all secondary orbital components that delivers the enhanced *endo* selectivity.

Conclusion

The effect of solvent on the activation energies and *endo/exo* selectivity on the four transition structures of the butadiene and acrolein Diels−Alder was studied. The microsolvation effect of explicit waters was found to induce a polarization of the transition structure, with a lowering of the activation barrier. The microsolvation of hydrogen bonding accounts for approximately one-half of the observed catalytic effect observed

(140) García, J. I.; Mayoral, J. A.; Salvatella, L. *Tetrahedron* **1997**, *53*, 6057.

by experiment. The macroscopic effects of solvation were studied by the implicit PCM model, which accounts for the remaining 50% of the experimental effect. The explicit hydrogen bonding is necessary to induce charge polarization of the NC transition structure and to allow enforced hydrophobic interactions and antihydrophobic effects. The full aqueous acceleration and enhanced *endo/exo* selectivity observed by experiment were only realized when solvation forces were approximated by the discrete-continuum model. The gas-phase activation energy was lowered to 11.5 kcal/mol, in excellent agreement with known experimental activation energies of similar Diels−Alder reactions in mixed methanol and water solutions. The computed *endo* preference was enhanced to 2.4 kcal/mol in aqueous solution. Specific polarization of the NC transition structure enhanced Singleton's [4+3] secondary orbital interaction, but all three independent interactions are necessary to explain the observed enhanced *endo* selectivity. We found that the *endo/exo* selectivity is equally influenced by both hydrogen bonding and bulk-phase effects. Therefore, the catalytic and *endo/exo* selectivity results are consistent with the hypothesis of maximum accumulation of unsaturation.

Acknowledgment. We thank IBM Corporation, the Department of Defense (DAAH04-96-1-0311 and DAAG55-98-1-0067), and the Arthur Vining Davis Foundations for financial support to make this research possible.

Supporting Information Available: Energies, zero-point energies, imaginary frequencies, and Cartesian Coordinates of all structures are available. This material is available free of charge via the Internet at http://pubs.acs.org.

JA0010249